MORPHOLOGICAL RESPONSES TO CALCIUM-INDUCED INTERACTION OF PHOSPHATIDYLSERINE-CONTAINING VESICLES

B. KACHAR,* N. FULLER,‡ AND R. P. RAND‡
*Laboratory of Neurobiology, National Institutes of Neurological and Communicative Disorders and Stroke, National Institutes of Health, Bethesda, Maryland, 20205; and ‡Department of Biological Sciences, Brock University, St. Catharines, Ontario, Canada L2S3A1

ABSTRACT Structural changes in phospholipid vesicles made of dioleylphosphatidylethanolamine (DOPE)/bovine phosphatidylserine (PS) (1/1, 3/1, 10/1) or of egg phosphatidylcholine (PC)/PS (3/1) and exposed to calcium chloride for various times have been observed by means of video-enhanced light microscopy and freeze-fracture electron microscopy. Calcium induces the formation of large, smooth double-bilayer diaphragms as the spherical vesicles adhere to and deform each other. No subsequent changes are seen with PC/PS vesicles. DOPE/PS vesicles respond to the resultant stress, with about equal probability, by either fusing, through diaphragm rupture, or deflating, by way of volume loss through intact bilayers, even when they contain up to 400 mM sucrose. The diaphragm areas only rarely show the structural destabilization necessary for fusion. The final state is lipid segregated into DOPE hexagonal and Ca-PS lamellar bulk phases with the exclusion of most of the vesicle contents. Results with these and pure PS vesicles studied earlier indicate that the early response of vesicles to calcium chloride is determined by the competing rates at which mechanical stress (bilayer tension and intravesicular pressure) builds up as the vesicles adhere and flatten against each other, and is relieved by vesicle fusion or by volume loss. We attribute the qualitatively different responses of these three lipid systems to their measured differences in adhesion energies and consequent rate of build-up of mechanical stress. Yield to that stress for any one of these lipid systems is not a unique sequence of morphological changes, and so it remains obscure how such a stochastic process could be used in the controlled process of cellular fusion.

INTRODUCTION

Secretion by exocytosis and myoblast fusion involves the controlled fusion of cell membranes. That control includes stable membrane apposition until fusion is triggered, transient destabilization and fusing of the membranes only in their areas of contact, and rapid return to stability. The trigger is usually associated with a rise in intracellular calcium ions and often with a rapid turnover of phosphatidylinositol. The focused destabilization and rupture ensures that the topological changes after fusion results in the mixing of only the correct aqueous compartments, so-called leakless fusion. That crucial transient stage is very rapid making it both improbable to capture morphologically and difficult to attribute to specific membrane components. Well-defined phospholipid bilayer systems continue to be used as models of membrane interaction and fusion to increase the probability of capturing the transient structures and to simplify the chemical complexity. In addition, lipids produced during phosphatidylinositol turnover, particularly diacylglycerol, are capable of disrupting bilayers (1) and may provide a possible link between the biochemical control of fusion and the physical chemical events of combining two membranes (2).

For such model systems to shed light on mechanisms relevant to the cellular process it is important to establish whether or not they mimic the topology of leakless fusion. Two morphologically distinct systems have been developed to assess this. In the first (3) the interaction of two populations of small (<300 A) or large (1,000 A) unilamellar vesicles is triggered by the addition of calcium chloride. Vesicle aggregation is measured by light scattering, mixing of their internal contents is measured by terbium-picolinic acid fluorescence, leakage is measured by release of carboxyfluorescne fluorescence quenching, and membrane mixing is measured by the mixing of fluorescent-labeled lipids (4). Changes characteristic of vesicle fusion, i.e., mixing of vesicle lipids and vesicle contents are, for most systems, associated closely in time with the release of vesicle contents. Usually the end state is the formation of bulk lipid phases (4). In the second system (5, 6), morphologically more akin to the cellular, multilayer phospholipid vesicles interact with a planar membrane. Fusion is assessed by the incorporation into the planar layer of specific ion-channel proteins and by the delivery of vesicle contents across the planar membrane. Separate adhesion and fusion steps have been detected (7). The fusion is triggered only after osmotic swelling of the adhered vesicles.

The morphological events in both these systems are surmised indirectly by reference to the reaction kinetics. Fundamental questions arise about those events and about their relevance to cellular fusion (8). For interacting spheres the question remains as to whether the fusion reaction and vesicle leakage are sequential in time and independant of each other, or whether each is an alternative initial reaction. For sphere-plane interactions the question remains as to whether osmotic rupture leads as well to release of vesicle contents without fusion with the planar membrane (7).

These two systems give different results with the same lipid and aqueous conditions (7, 9, 10). For example with phosphatidylethanolamine/phosphatidylserine (PE/PS) mixtures interacting spheres destabilize on calcium addition but sphere-plane interactions are stable unless stressed osmotically. Again interacting spheres of neutral lipids never destabilize but sphere-plane bilayers do so if stressed osmotically. These differences highlight the importance of the different mechanical constraints and stresses of the bilayers (sphere-sphere vs. sphere-plane) during their interaction. What has not been widely recognized are the mechanical consequences of imposing strong attraction between bilayer membranes (11). In both systems it appears that increasing bilayer stress to rupturing levels is required to trigger a response. We attempt here to make direct morphological measurements of interacting vesicles and to relate these to the more indirect studies and to the known mechanical properties of bilayers.

We have previously visualized directly, by light and electron microscopy (12), the response of calcium-induced interaction of large PS vesicles. The initial reaction of these vesicles is to flatten against each other, forming a double bilayer diaphragm. They yield to the resultant stress by rupture of either the diaphragm (fusion) or of the bilayer outside it (leakage). Diaphragm rupture was only so frequent as to make the fusion and leakage response about equally probable. High-resolution freeze-fracture electron microscopy revealed no clue to the nature of the defect formation that results in bilayer destabilization and rupture. Here we have attempted to seek lipid species and aqueous conditions that might lead to focusing the destabilizing reaction in the area of contact so that the fusion reaction predominates. We have shown that stress created by Ca-induced adhesion of vesicles containing diolylphosphatidylethanolamine (DOPE) and bovine brain PS is released either by diaphragm rupture and fusion or by volume loss, but rarely with vesicle rupture. Ultimately this system decayed to separate bulk lipid phases characteristic of DOPE and PS-Ca. Phosphatidylcholine (PC)/PS vesicles, on the other hand, attain stable adhesion on calcium addition without fusing and without apparent volume loss. We attribute these different responses to measured differences in the interaction energies of the different lipid species.

MATERIALS AND METHODS

Lipid and Vesicle Preparation

Bovine brain PS, egg PC, and DOPE were obtained from Avanti Polar Lipids, Inc. (Birmingham, AL). The PS mixed at 30 wt% in water formed two lamellar phases, as indicated by x-ray diffraction, of repeat spacings d = 55 Å, characteristic of the Ca-PS phase (13) and d = 95 Å, characteristic of swelled charged bilayers (14). This lipid was converted to the sodium salt using a chloroform-methanol-aqueous two phase system after which the Ca-PS phase disappeared and all the lipid behaved as charged lipid. Thin-layer chromatography showed the lipids to be >99% pure. They were stored dry under nitrogen at −60°C. Defined mixtures of lipids were formed by combining chloroform solutions of known composition, removing solvent by rotary evaporation and then vacuum drying.

Giant complex vesicles (GCV) were produced by overnight hydration of 10 mg lipid in 10 ml 2 mM TES buffer (pH 7.4) followed by gentle vortexing until a visibly uniform suspension was attained. We have called these GCV because they are several microns in diameter and they can be oligolamellar and/or contain several small freely diffusing vesicles (12). Large unilamellar vesicles (LUV) were formed by the reverse evaporation phase method of Sozka et al. (15) using 10 mg. lipid/mililiter solution of the TES buffer. The final sizing was done by filtering through either a 1 or 0.1 μm Nucleopore membrane.

Video-enhanced Differential Interference Contrast Microscopy

For the light microscopic observations, a solution of GCV was placed on a shallow chamber, between a microscopic slide and a coverslip. $CaCl_2$ was added by placing a small concentrated drop (60 mM) through a side opening. Preparations were observed with an ICM inverted microscope (Carl Zeiss Inc., Thornwood, NY) equipped for differential interference contrast (DIC), with an oil immersion 1.4 NA condenser and 1.3 NA plan APO 100 × objective. A dramatic improvement in the performance of the DIC microscope is obtained when the image is viewed with a high-resolution video system (16). The video camera was a Chalnicon camera driven by a polyprocessor frame memory (model C-1000; Hamamatsu Systems, Inc., Waltham, MA). At high video gains a mottle pattern appeared in the background due to unavoidable dirt and imperfections in the lenses (16). The frame memory was used to subtract this pattern continuously from succeeding frames. The magnification of the images seen on a 19-inch monitor was 10,000 × and represented an optical section ~0.2 μm thick.

Rapid-mixing, Spray-freezing, Freeze-fracture Electron Microscopy

Rapid spray-freezing of LUV and GCV without cryoprotectant was done on standard Balzers equipment. However, before freezing the vesicle suspension was very rapidly mixed (milliseconds) with an equal volume of a second solution using a Berger ball mixer (Commonwealth Technology Inc., Alexandria, VA) (12). The second solution contained 10 mM $CaCl_2$ in the vesicle medium, which on rapid mixing became 5 mM. Freezing was accomplished at a series of intervals down to ~100 ms after mixing (12). The freeze fracturing was done on Balzers 400T equipment, (Hudson, NY) with both cleaving and quartz-crystal monitored shadowing (45°) and replicating at 5×10^{-8} mbar and −150°C.

X-ray Diffraction

Structural determination of the lipid systems were also investigated using standard x-ray diffraction methods (2). Lipid, ~1 h after addition of $CaCl_2$, was collected by centrifugation and sealed between mica windows one millimeter apart. X-ray diffraction by slit collimated, quartz crystal

monochromatic radiation (λ = 5.401 A) was recorded photographically. The lipid structure was determined as multilamellar by a series of discrete reflections of integral orders of the lamellar repeat dimension, as hexagonal by a series of discrete reflections of dimension d, $d/\sqrt{3}$, $d/\sqrt{4}$, $d/\sqrt{7}$, etc., or as amorphous if only central scattering and no discrete reflections were observed. The coexistence of more than one phase was detected by a combination of reflections for each.

OBSERVATIONS

The video light microscopy shows the sequence of events that occurs for individual vesicle interactions on Ca addition. They were determined in many experiments involving several hours of recording. Not all topological events could be defined since the optical section is so thin, or the vesicle suspension in some areas too complex, or some events too fast. We describe below all the different sequential events that could be defined unambiguously and analysed from video recording with frame-by-frame analysis. The electron microscopy on the other hand provides high-resolution static images of the vesicles and their bilayers at precise times after Ca addition. Hundreds of fields were examined and the earliest events of vesicle interaction defined. In the case of DOPE/PS vesicles many structures that formed at later, intermediate, times were too complex to be defined unambiguously, although bilayer structure and contact areas could be seen at high resolution. Final equilibrium structures could be interpreted unambiguously both by electron microscopy and by x-ray diffraction.

Light Microscopy

On addition of 60 mM $CaCl_2$ a wave of changes passes through the GCV suspension in the form of a moving front. Ahead of the front no vesicle interactions have occurred. Well behind the front events have finished. As the front advances and the $CaCl_2$ is diluted vesicle interactions are slower. One could thus select areas of the field according to the stage and rate of vesicle interaction events.

Contacting or colliding DOPE/PS spherical vesicles, with variable delays (1–10 s) after $CaCl_2$ arrival, rapidly (<1/60 s, the duration of a video field) flatten against each other forming large areas of contact (Fig. 1 *a*, *d*). Subse-

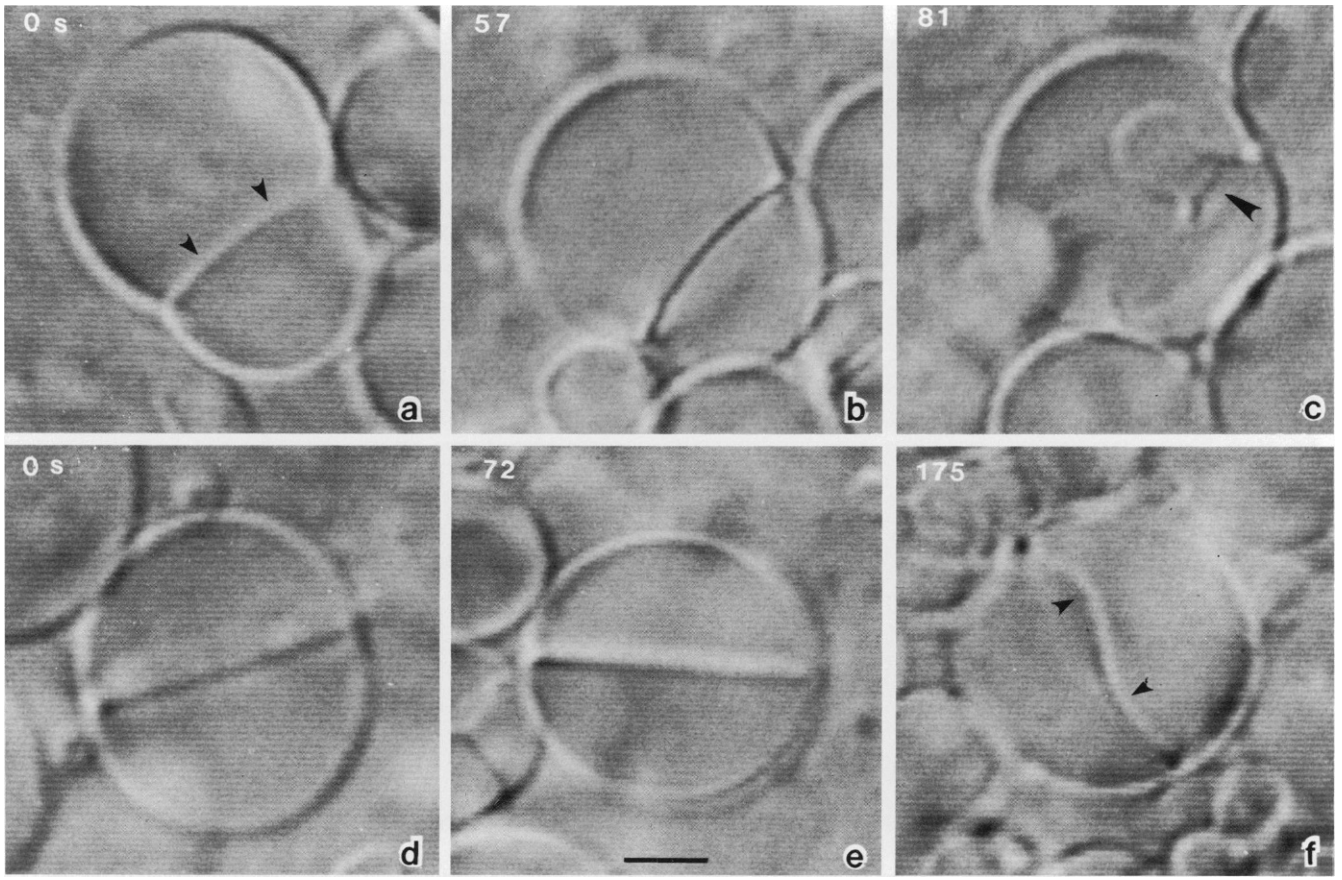

FIGURE 1 Still frames of video-enhanced differential interference contrast images of Ca-induced interactions between giant oligolamellar DOPE/PS (3/1) vesicles. Numbers in white indicate time (in seconds) elapsed between frames. Contacting spherical vesicles form flat areas of contact after a variable delay in *a* (*arrowheads*) that persist for seconds to minutes. The diaphragm area increases as the vesicles adhere (*a–b*). Part *c* shows the formation of an invagination (*arrowhead*) in the inner vesicle, contained in one of the interacting vesicles, that was squeezed during the flattening of the two vesicles against each other. *d–f* show progressive enlargement of the diaphragm area between two interacting vesicles until the adhered pair is spherical in shape. In *f* the diaphragm (*arrowheads*) overgrows the diameter of the adhered pair to become wrinkled. The bar represents 1 μm.

quently, but again with highly variable delays (one to many seconds) one of two qualitatively different events ensues. In one the contacting, vesicles slowly collapse against each other with an enlargement of the contacting area (Fig. 1) until the resultant combination is about spherical in shape. The contacting area forms a diaphragm that separates the two original compartments. No such reaction within vesicles is observed, indicating that calcium does not reach the interior. Vesicle deformation and diaphragm growth in oligolamellar vesicles (vesicles with more than one bilayer envelope) causes folding or invaginations of the inner layers (Fig. 1 *c*). Often the diaphragm continues to expand thus overgrowing the diameter of the spherical combination of vesicles and becomes irregular (Fig. 1 *d–e*). Estimates of areas and volumes in that sequence, on the assumptions that the vesicles are portions of spheres and that the images are optical sections through the vesicle center, show the bilayer areas remain constant as the volumes decrease, one by 14% and the other by 28%. Deviation from those assumptions could introduce large errors in these estimates. Nevertheless the qualitative observation of volume loss and large excess area over that of a sphere is clearly shown by the final spherical configuration shown by the two vesicles in Fig. 1 *f*.

An alternative response to the initial vesicle contact and adhesion is that as the area of contact between interacting vesicles suddenly ruptures, a single vesicle forms and the contents of the two vesicles mingle (Fig. 2 *a–c*). These fusion reactions, characterized by the sudden breakage of the diaphragm and the visualization of content mixing, was often observed when at least one of the interacting vesicles was multilamellar or contained a high density of smaller vesicles (Fig. 2 *d–f*).

Observations in many experiments revealed that these configurations, fused or collapsed vesicles, then remained for a long time (many seconds to minutes). Still no reaction within vesicles is observed over this time, indicating that $CaCl_2$ does not reach the interior. Within this time very few (<1%) vesicles rupture with release of vesicle contents to the external medium. Eventually however most of the lipid collapses into large compact aggregates. These aggregates with time (hours) show two distinct birefrigent

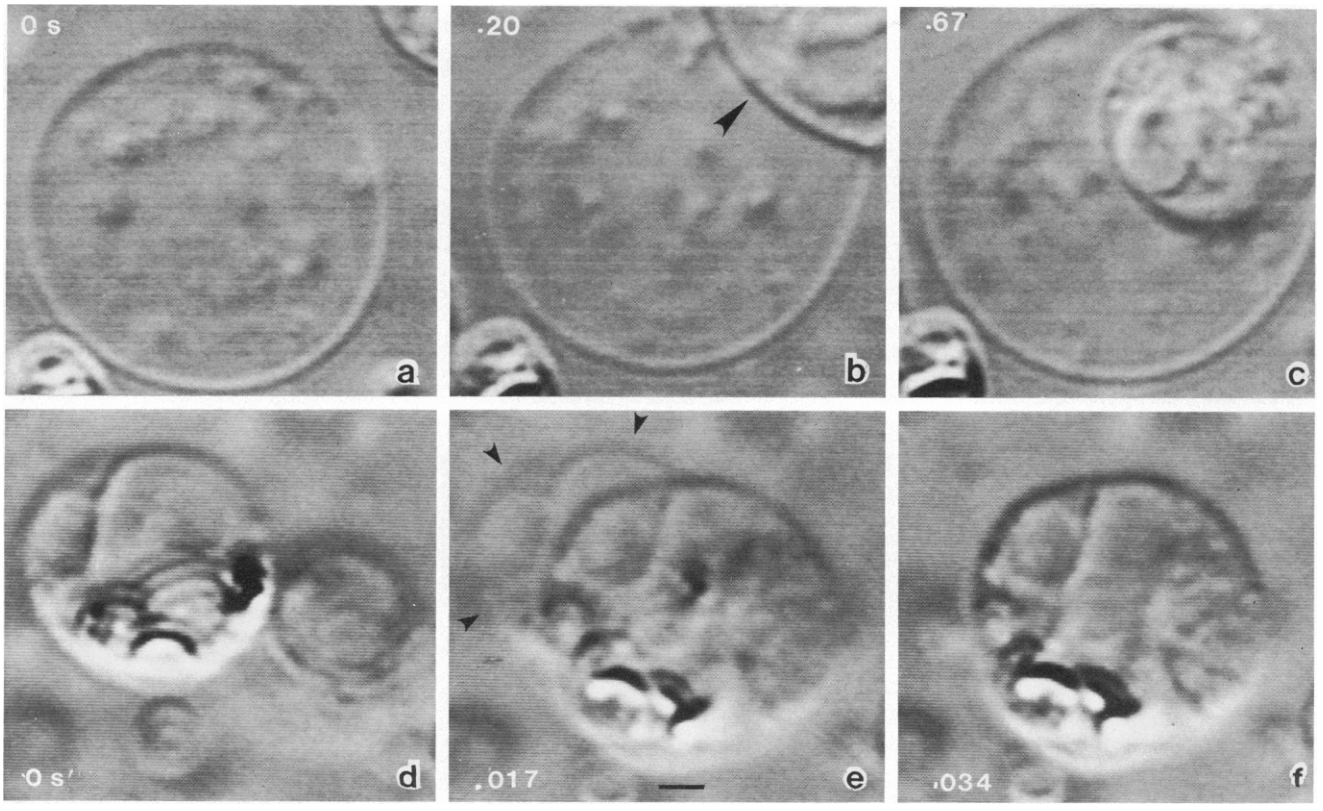

FIGURE 2 The *a–c* sequence of still pictures shows vesicle interaction in the presence of calcium chloride that results in fusion. In the top right corner of *a* the partially visualized multilamellar vesicle approaches a larger stationary vesicle (in the center of the field). The interaction results in the sudden formation of a diaphragm (*arrowheads*) that lasts for a short time and suddenly ruptures with communication of contents of the interacting vesicles (*c*). There is no apparent volume loss since the diameter of the smaller vesicle (preserved by inner membrane layers of the multilamellar complex) that was incorporated in the fused pair is the same as its original diameter. The curvature of the diaphragm (at the arrowhead in *b*) is not the diameter of the smaller vesicle but an angular view of the perimeter of the flat diaphragm. Figs. *d–f* show consecutive video fields (1/60-s intervals) of GCV prepared in the presence of 1 M sucrose and diluted with a calcium chloride solution. In *d* two individual vesicles have not interacted, but in the subsequent video field (17 ms later) they have already interacted and fused. A ghost of one of the original vesicles (*small arrowheads*) is recorded overlapping the image of the interacted pair during the interlaced line scanning of the video frame. The bar represents 1 μm.

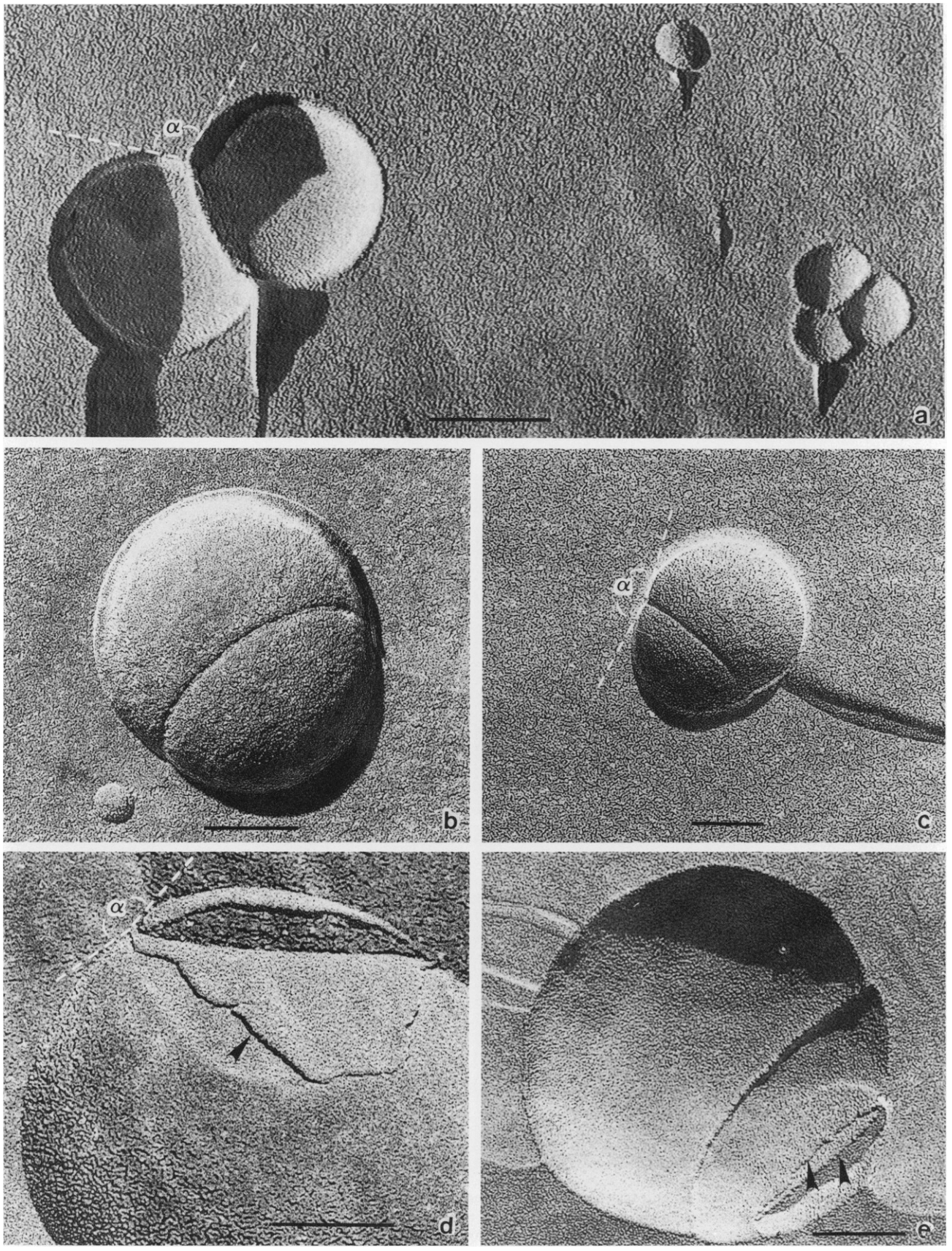

FIGURE 3 Freeze-fracture of fast frozen, rapid mixed DOPE/PS vesicles showing the earliest changes (100 ms) after the addition of 5 mM $CaCl_2$. Aggregation of two or more vesicles (*a*) produces large areas of contact or diaphragms. Within this time interacting vesicles were arrested at different degrees of vesicle deformation (*a–d*). Although the sum of the two angles of contact is often $<180°$ (*a*), frequently that angle attained 180° (*c*). All diaphragms appear to be made of two tightly apposed bilayers (*arrowheads* in *d* and *e*). Vesicles in *b* and *e* were prepared in the presence of 100 mM sucrose and vesicles in *c* were prepared in 400 mM sucrose. The bars represent 1,000 Å.

domains. X-ray diffraction of this material showed the coexistence of a lamellar phase of repeat spacing d = 55 Å and a hexagonal phase with fundamental spacing of 64.5 Å. The former is characteristic of a pure Ca-PS phase (14). The latter is characteristic of fully hydrated DOPE (17). This shows that calcium in time induces the segregation of these two lipid species as the vesicles collapse and form the final aggregates.

When GCV's were prepared in 1 M sucrose solution and mixed with the $CaCl_2$ solution the fusion reaction occurs more rapidly on vesicle contact (Fig. 2 *d–f*). Vesicle deformation could not be seen since both interaction and fusion occurred within a video field (1/60 s).

Electron Microscopy

DOPE/PS Vesicles. Before the addition of calcium chloride vesicles were all isolated, smooth and spherical, like those in Fig. 3 except no adhering vesicles were observed. Within 100 ms after rapid mixing with 5 mM $CaCl_2$ many vesicles had aggregated and were arrested in different degrees of deformation (Fig. 3 *a–e*). Consequently the relative area of contact varies a lot. However all areas of contact were smooth, double-bilayer diaphragms (Fig. 3 *d, e*). Although the sum of the two angles of contact between diaphragm and vesicle is often <180° (Fig. 3), frequently a 180° angle is attained with extensive loss of volume at these early times. Cross-fractures of two such collapsed adhering vesicles are seen in Fig. 3 *d, e*, in each case the smaller adhered vesicle has lost most of its volume as it flattens against the larger vesicle. Volume loss occurs even in experiments where the vesicles contained 100 mM sucrose (Fig. 3 *b, e*) or 400 mM sucrose (Fig. 3 *c*).

All the images described thus far are consistent with the maintenance of the surface topology that defines the

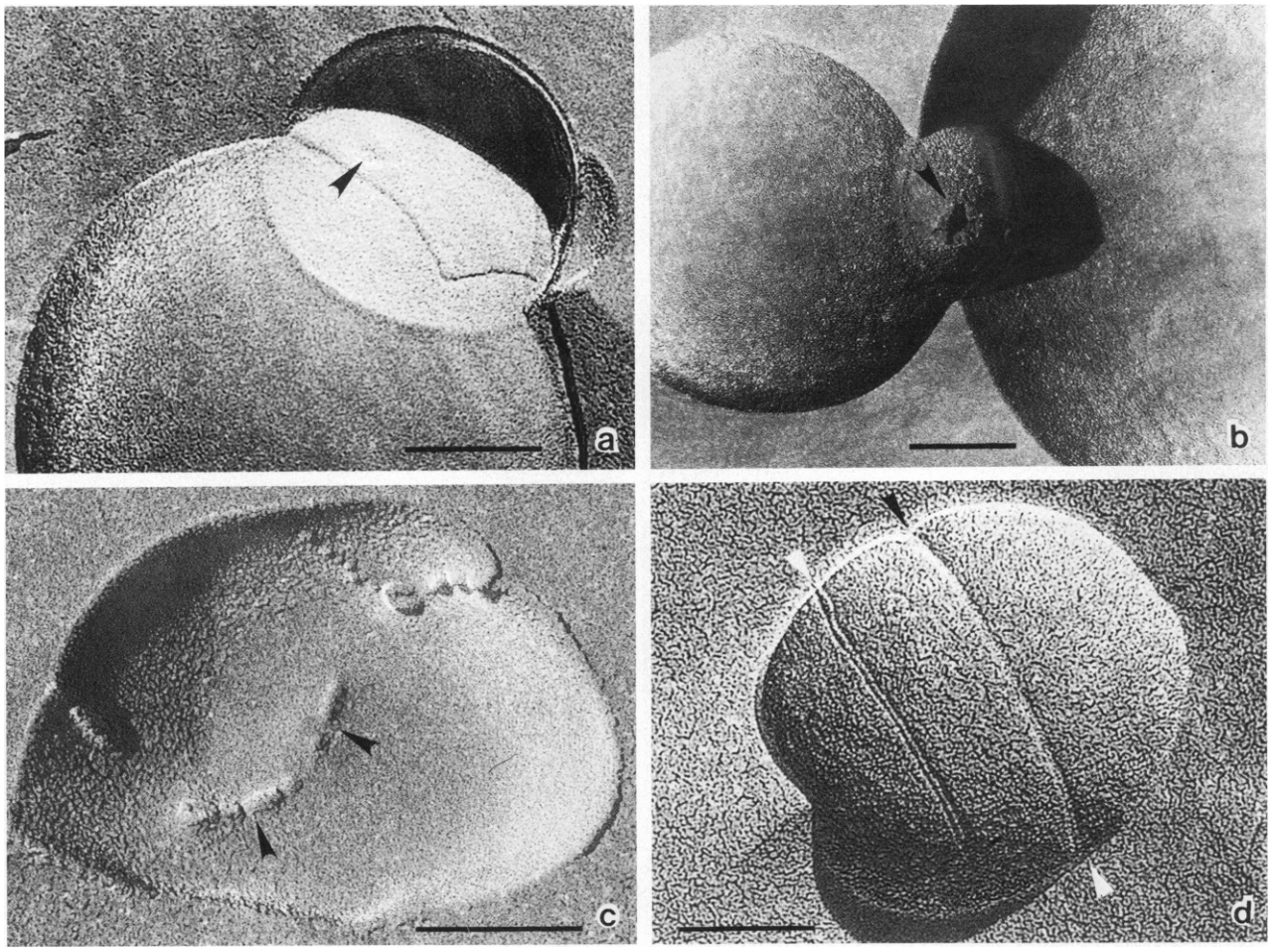

FIGURE 4 Freeze-fracture of fast-frozen, rapid-mixed DOPE/PS vesicles. (*a*) Defects (*arrowhead*) occasionally can be seen on the double bilayer diaphragms between Ca-induced interacting vesicles at early times (100 ms). (*b*) The *arrowhead* points to a defect that suggests a partially ruptured diaphragm. Part *c* shows discontinuous linear arrays of high curvature structures suggestive of edges of exploded diaphragms. These structures could represent totally ruptured diaphragms corresponding to the vesicle fusion. Part *d* shows "en face" views of the region of interaction between vesicles. When the contact angles sum to <180° the line of interaction between the fracture face of the two adjacent vesicles is a single groove (black *arrowhead*). When that angle is close to 180°, the line of contact appears as double grooves separated by a 100-Å ridge (white *arrowheads*). The bars represent 1,000 Å.

segregation of the inside and outside aqueous compartments of the vesicles; i.e. no bilayers are ruptured. However in about half of the images of adhered vesicles continuity of the contacting membranes is lost. In such cases discontinuous linear arrays of high curvature structures, suggestive of the linear arrays of diaphragm edges, are the only signals of vesicle boundaries (Fig. 4 *c*). These structures likely represent remnants of totally ruptured diaphragms corresponding to vesicle fusion with communication of vesicle compartments, as was observed in the video light microscopy. Very rarely (<1%) defects within the smooth double-bilayer diaphragms between interacting vesicles are observed (Fig. 4 *a*); and in some cases indication of an early stage of rupture of the diaphragm is evident (Fig. 4 *b*).

Particularly prominent and the only nonbilayer structures in these interacting vesicles are the very narrow curved linear images of the edges of diaphragms seen on contiguous fracture faces of the membranes of interacting vesicles. When seen on the *P* face or inside monolayer of vesicles with contact angles <180° these lines are a single groove (Fig. 3 *b*, *c*). When seen on vesicles with contact angles of 180° they are double grooves separated by a 100-A ridge (Fig. 4 *d*). We interpret the latter as resulting from fusion of the outer monolayers at the edges of the diaphragm (12). Such hemifusion would inhibit further growth of the diaphragm, stabilizing the configuration of the adhered vesicles.

At 20–30 s after calcium addition no new configurations of vesicle or new structures are seen, although in large aggregates some structures were difficult to define. Note that at this time some observed vesicles may have been in contact a maximum of 30 s, but some may have made contact just before freezing. Nevertheless any new structural configurations that form subsequent to those already described must form considerably more slowly since none were seen at this time.

Approximately one hour after mixing, hexagonal phase lipid, lamellar phase lipid, and aggregates of collapsed vesicles were observed by electron microscopy. The first two structures were confirmed by x-ray diffraction of the rapid-mixed sample.

No measurable differences in vesicle response or in this sequence of events or in the proportion of fused and collapsed vesicles were detected for vesicles composed of DOPE/PS 1/1, 3/1, or 10/1.

Egg PC/PS Vesicles. Although isolated egg PC/PS (3/1) vesicles appear by electron microscopy identical to the PE/PS vesicles before mixing, their behavior on addition of calcium chloride was qualitatively different. Calcium chloride (5 mM) induced the formation of large aggregates of adhering vesicles that did not apparently fuse or lose volume. Areas of contact were smooth flat double-bilayer diaphragms. No subsequent morphological change was detected up to several hours after adhesion (Fig. 5).

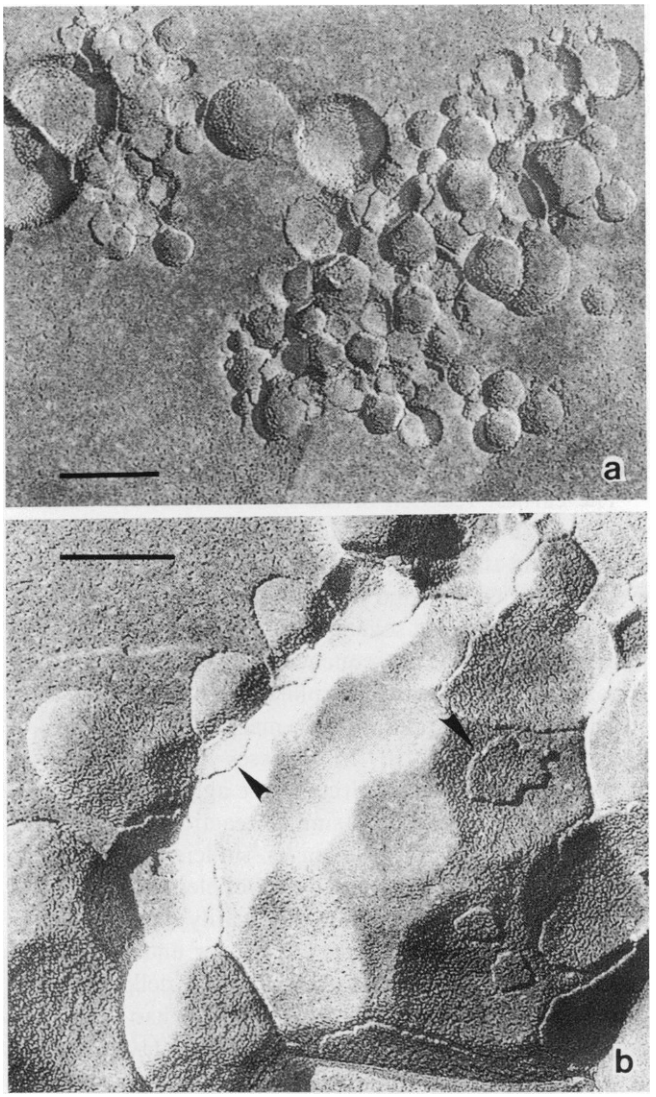

FIGURE 5 Equilibrium state of interacting PC/PS vesicles after addition of 5 mM $CaCl_2$. The vesicles in *b* are much larger as they were filtered through a 1 μm Nucleopore filter. The vesicles interact to form large aggregates by stable adhesions between vesicles *a*. Areas of contact are smooth flat double bilayer diaphragms (*arrowheads a, b*). The bars represent 1,000 Å.

X-ray diffraction of such aggregates show only central scattering characteristic of the amorphous structure of these aggregates and the absence of multilamellar phase lipid.

DISCUSSION AND CONCLUSIONS

Our major objective in using these experimental strategies was to provide direct evidence of the morphological changes and their time course that phospholipid vesicles are triggered to undergo by calcium. The most important lessons we learn from these studies are qualitative, and are that the changes beyond vesicle adhesion are neither a unique sequence of events nor, in spite of our efforts, synchronous. Two distinct observations show this. First the light microscopy shows that after DOPE/PS vesicles interact to the extent of forming double bilayer diaphragms

either of two different events ensues; the vesicles either fuse or they remain adherent and lose volume. Second, for several neighboring pairs of vesicles the time between calcium arrival and the rapid formation of a diaphragm is highly variable, as is the time between diaphragm formation and subsequent fusion or volume loss. These variable delays destroy any synchrony of events that might ensue after calcium arrival. Electron microscope images showing various stages of vesicle interaction after rapid mixing are consistent with both the nonuniformity and asynchrony of response. Consequently our original objective of obtaining a quantitative description of a single well-timed sequence of events is largely precluded. This has important implications, where interpretations of data using more indirect methods invoke or assume a uniform sequence of events.

The earliest reaction of the vesicles to added calcium was their mutual adhesion. Subsequent morphological changes and their estimated time course in the two lipid systems studied here and the PS system studied previously (12) are summarized schematically in Figs. 6 and 7. Our interpretation of the consequences of the adhesion reaction is based on the observed morphology, on previously measured adhesion energies, and on mechanical properties of bilayer vesicles (11, 18). In all cases flat double-bilayer areas of contact form resulting in the aggregation of from two to several vesicles. No similar reactions are observed within vesicles. The adhesion is sufficiently strong to deform the spherical shape as the vesicles flatten against each other. Such deformation necessarily increases intravesicular pressure and places the bilayer under increased tension. It has been shown by Evans and his colleagues that bilayer tensions and area increases greater than ~3 dynes/cm and 3%, respectively (11, 18) result in bilayer rupture. If low-adhesion energies result in tensions below this critical level, stable adhesion and aggregation of vesicles could result. Such is observed for the PC/PS vesicles. If the adhesion energy and consequent vesicular pressure and bilayer tension are high, such stresses may be relieved in two qualitatively different ways. In one the contact area could break and the vesicles fuse into a combination whose area/volume ratio becomes high enough that the stress is removed. In the second, volume loss could relieve the tension in the stressed bilayer. Both responses have been observed and each leads to a qualitatively different outcome for the vesicles.

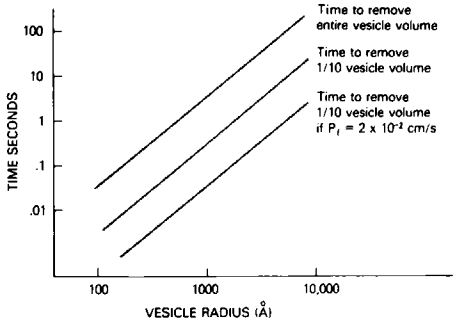

FIGURE 6 Times for deflation of phospholipid vesicles when their contents are placed under pressure. Rate of water flow J (cc/s) through bilayer membranes of area A (cm^2) with water permeability coefficient P (cm/s) is given by $J = A \times \upsilon \times P \times P/R \times T$, where υ is the partial molar volume of water (18 cc/mol), R the universal gas constant and T absolute temperature (7). Time is for loss of the indicated fraction of vesicle contents when they are stressed to produce pressures resulting from bilayer tensions of 3 dynes/cm and with $P = 2 \times 10^{-3}$ cm/s (upper two lines), the permeability coefficient of unstressed bilayer membranes (7). The lower line applies to the case where the permeability is increased by an order of magnitude, which may occur for such highly stressed bilayers.

Both such stress-relieving mechanisms are seen in vesicles of DOPE/PS and of pure PS. Rupture of the contact area results in vesicle fusion and this is observed in roughly one half of the responses. Volume loss however is by two quite different ways. With pure PS vesicles we observed by light microscopy the rapid rupture and disappearance of one of the adhering vesicles (12). With DOPE/PS vesicles volume loss is not by vesicle rupture but is more controlled by leakage of contents through the stressed but intact bilayers. The contact area grows and volume loss continues even after the combination of vesicles attains a spherical shape. The diameter of the diaphragm can exceed the cross-sectional area (Fig. 1 *f*) of that sphere and total collapse may ensue (Fig. 3 *d*, *e*).

We suggest that these two different pathways of volume loss result from differences in the competing rates of increase in vesicle stress and of relief of that stress. Our observations of PS vesicle rupture showed that critical tension was always reached before volume loss through intact bilayers could reduce it (12). On the other hand with DOPE/PS vesicles volume loss through intact bilayers relieves vesicle stress before rupture tensions are reached. We interpret that more moderate response as a result of DOPE/PS bilayers having reduced adhesive energies and/or increased permeability, both would result in slower production of bilayer tension allowing more time for volume loss to relieve the stress before rupture tensions are achieved. Calcium-induced adhesion of PC/PS vesicles is apparently so weak that vesicle deformation does not produce significant bilayer stress or volume loss and stable adhesion results. In sum we conclude that the three lipid systems show three different responses as a result of three different levels of adhesion energy induced by calcium addition.

How does calcium induce these different adhesion energies? Calcium can enable adhesion three ways, by screening electrostatic repulsion, by binding to PS reducing surface charge density, and by forming PS-Ca-PS *trans*-complexes between the outer monolayers of adhering vesicles. We have estimated that the affinity for calcium of pure interacting PS vesicles is so high that adhesion energies would produce resultant tensions that far exceed critical levels if no volume loss results (19). We suggest such tensions are induced by calcium in PS vesicles, and certainly such Ca-PS-Ca complexes appear to form very

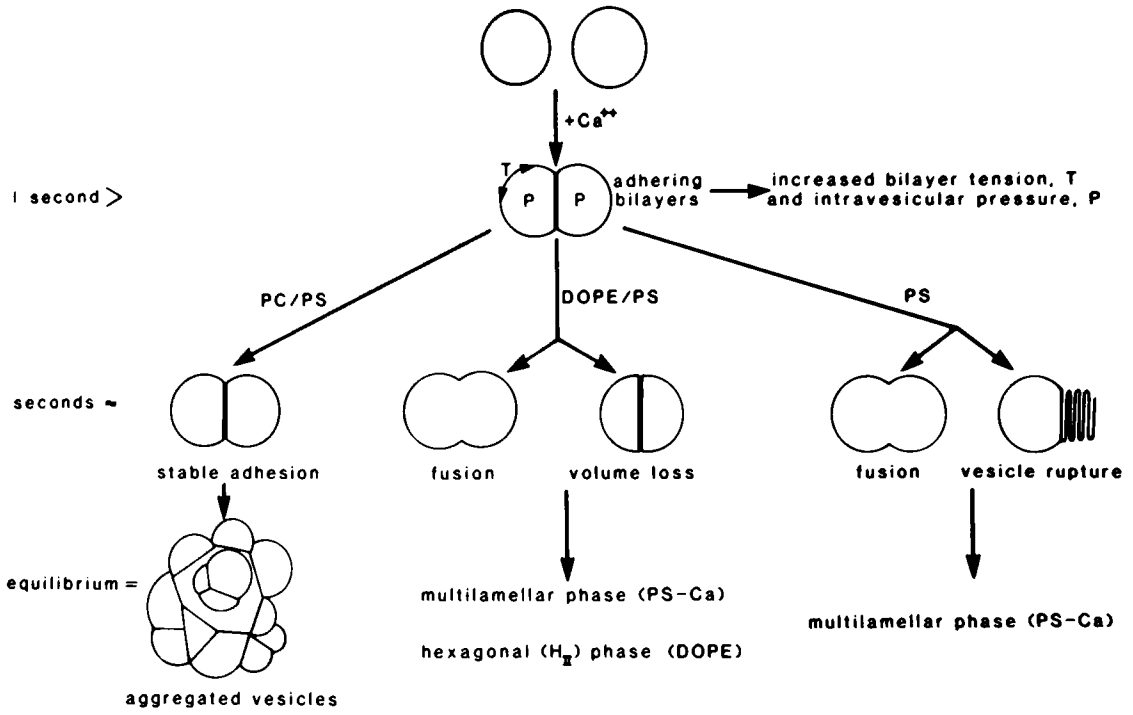

FIGURE 7 Schematic diagram of the morphological consequences of Ca-induced interaction of the three kinds of vesicles studied. Transient states between seconds and equilibrium were too complex to be defined. Weak interactions (PC/PS) lead to simple adhesion of the vesicles. Stronger interactions (DOPE/PS) lead to either fusion or deflation of the adhered vesicles and eventual segregation of the lipids. Strongest interactions (PS) lead to either fusion or violent rupture of the vesicles and eventual formation of the dehydrated Ca-PS lamellar phase.

early in the process of PS vesicle destruction (12). For bilayers containing DOPE and PC, however, such complexes are not observed. Reduction of electrostatic repulsion by calcium would leave intact the strong hydration repulsion that has been measured for these neutral lipids (20). We have measured by x-ray diffraction of these specific lipids that hydration repulsion alone prevents bilayers from approaching closer than ~12 Å for DOPE and 27 Å for PC. These distances would, in the case of DOPE, inhibit or, in the case of PC, preclude the formation of PS-Ca-PS *trans* complexation between these vesicles. Furthermore, the difference in behavior between DOPE- and PC-containing vesicles lies in their different adhesion energies. Both for multilayers (14, 19) and for vesicles (21) those energies are about an order of magnitude greater for PE than PC, 10^{-2} and 10^{-1} erg/cm^2, respectively (19). PE-containing vesicles adhere strongly enough to cause deformation and intravesicular pressure that induces the volume loss we observe. PC-containing vesicles, on the other hand, adhere so weakly as to achieve equilibrium aggregation without consequent destruction.

We have attempted to estimate the rate of vesicle volume loss through intact bilayers for the response of the DOPE/PS vesicles. Fig. 6 gives the times expected for the specified fractional volume loss as it varies with vesicle size, for bilayer tensions of the maximum allowable 3 dynes/cm and under the conditions specified in the figure. LUV are expected to deflate much faster than GCV, and the estimates serve to indicate that the times of deflation are within the range of observed times, milliseconds for LUV and many seconds for GCV. However it should be emphasized and it is important to realize that most of the factors contributing to rate of volume loss are themselves changing during the process. The energy of interaction (11), the area of contact and the bilayer tension all grow as the vesicles deform (19). Consequently, for example, bilayer permeability must change during the process. It would appear from the highly deflated vesicles of Fig. 3 *d*, *e* that even sucrose permeability must reach high values in such stressed bilayers. Furthermore relative sizes and initial tension of the vesicles even before interaction cannot be controlled.

These results agree in some respects with the indirect measurements of vesicle fusion by fluorescence assay (4). Thus rapid fusion is observed with PS and DOPE/PS vesicles, but is precluded with vesicles containing the levels of PC used in this study (9). Fusion of these latter vesicles with planar membranes, however, can occur only if accompanied by the disruptive force of osmotic swelling (10). Taken together these results suggest that in all cases mechanical bilayer tension and not enhanced contact alone is required to trigger the bilayer destabilization leading to fusion or bilayer rupture. Even the incorporation of large amounts of the nonbilayer forming lipid DOPE is not sufficient to make fusion the dominant reaction after vesicle adhesion.

Responses of DOPE/PS vesicles subsequent to the early events just described are too complex to analyze further. They would result from interactions of two different populations of vesicles, those that have fused and those that have deflated. The final equilibrium state of all these systems are nevertheless characterized unambiguously with only the PC/PS vesicles having any resemblance to the original state with some retention of their aqueous contents.

The present results differ with the interpretation of the fluorescence assays that fusion and then leakage are sequential events when two vesicles interact. These direct observations show that after initial contact either fusion or leakage are about equally likely events. Our results also show the possibility of volume loss that may go undetected in the fluorescence assay depending upon the permeability of the stressed bilayer.

In spite of a high proportion of images containing large areas of contacting bilayers, only rare examples of bilayer destabilizations leading to diaphragm rupture and fusion were detected (Fig. 4 *a*, *b*). Their rarity shows them to be very short-lived in time. This is consistent with the light microscopy that showed that diaphragms could last many seconds, but that their rupture and disappearance took place in <17 ms. Furthermore, bilayers containing 90 mol% DOPE, a lipid that itself does not self-assemble into bilayers, can, form featureless adhering bilayers. Thus there is no indication what role lipidic particles (22), whatever their structure (23), play in the interaction process. The calculations of Siegel (23) suggest their lifetime may be too short in this system to be detected. Others have shown their appearance to arise a long time after the initial contacts and responses are over (24).

In conclusion, we attribute the morphological responses after Ca-induced interaction of spherical vesicles to the consequent mechanical stresses that build up in the bilayers. These stresses are directly related to known intervesicle adhesion energies and are identical to those that would result from osmotic stress. Where stresses reach critical levels, either fusion or volume loss results. If indeed such a stochastic process is used in the control exhibited in cellular fusion, it remains entirely obscure how the yield to stress is restricted to the contact region.

B. Kachar acknowledges the continuous support of Dr. T. S. Reese, R. P. Rand acknowledges the financial support of the Natural Sciences and Engineering Council of Canada.

REFERENCES

1. Das, S., and R. P. Rand. 1985. Diacylglycerol causes major structural transitions in phospholipid bilayer membranes. *Biochem. Biophys. Res. Commun.* 124:491–496.
2. Das, S., and R. P. Rand. 1986. Modification by diacylglycerol of the structure and interaction of various phospholipid bilayers. *Biochemistry*. In press.
3. Wilschut, J., N. Duzgunes, R. Fraley and D. Papahadjopoulos. 1980. Studies on the mechanism of membrane fusion: kinetics of calcium ion-induced fusion of phosphatidylserine vesicles followed by a new assay for mixing of aqueous vesicle contents. *Biochemistry*. 19:6011–6021.
4. Wilschut, J., N. Duzgunes, K. Hong, D. Hoekstra, and D. Papahadjopoulos. 1983. Retention of aqueous contents during divalent cation-induced fusion of phospholipid vesicles. *Biochim. Biophys. Acta*. 734:309–318.
5. Zimmerberg, J., F. S. Cohen, and A. Finkelstein. 1980. Fusion of phospholipid vesicles with planar phospholipid bilayer membranes. I. Discharge of vesicular contents across the planar membrane. *J. Gen. Physiol.* 75:241–250.
6. Cohen, F. S., J. Zimmerberg, and A. Finkelstein. 1980. Fusion of phospholipid vesicles with planar phospholipid bilayer membranes. II. Incorporation of a vesicular membrane marker into the planar membrane. *J. Gen. Physiol.* 75:252–269.
7. Akabas, M. H., F. S. Cohen, and A. Finkelstein. 1984. Separation of the osmotically driven fusion event from vesicle-planar membrane attachment in a model for exocytosis. *J. Cell Biol.* 98:1063–1071.
8. Rand, R. P., and V. A. Parsegian. 1986. Mimicry and mechanism in phospholipid models of membrane fusion. *Annu. Rev. Physiol.* 48:201–212.
9. Duzgunes, N., J. Wilshut, R. Fraley, and D. Papahadjopoulos. 1981. Studies on the mechanism of membrane fusion: role of head group composition in calcium- and magnesium-induced fusion of mixed phospholipid vesicles. *Biochim. Biophys. Acta*. 642:182–195.
10. Cohen, F. S., M. H. Akabas, J. Zimmerberg, and A. Finkelstein. 1984. Parameters affecting the fusion of unilamellar phospholipid vesicles with planar bilayer membranes. *J. Cell Biol.* 98:1054–1062.
11. Evans, E. A., and V. A. Parsegian. 1983. Energetics of membrane deformation and adhesion in cell and vesicle aggregation. *Ann. NY Acad. Sci.* 416:13–33.
12. Rand, R. P., B. Kachar, and T. S. Reese. 1985. Dynamic morphology of interacting phosphatidylserine vesicles. *Biophys J.* 47:483–489.
13. Rand, R. P., and V. A. Parsegian. 1984. Physical force considerations in model and biological membranes. *Can. J. Biochem. Cell Biol.* 62:752–757.
14. Rand, R. P. 1981. Interacting phospholipid bilayers: measured forces and induced structural changes. *Annu. Rev. Biophys. Bioeng.* 10:277–314.
15. Szoka, F. C., and D. Papahadjopolous. 1978. Procedure for preparation of liposomes with large internal aqueous space and high capture by reverse-phase evaporation. *Proc. Natl. Acad. Sci. USA*. 75:4195–4198.
16. Allen, R. D., and N. S. Allen. 1983. Video-enhanced microscopy with a computer frame memory. *J. Micros. (Oxf.)*. 129:3–17.
17. Kirk, G. L., and S. M. Gruner. 1985. Lyotropic effects of alkanes and headgroup composition on the L-H liquid crystal phase transition: hydrocarbon packing vs. intrinsic curvature. *J. Phys.* 46:761–769.
18. Evans, E., and R. Kwok. 1982. Mechanical calorimetry of large dimyristoylphosphatidylcholine vesicles in the phase transition region. *Biochemistry*. 21:4874–4879.
19. Parsegian, V. A., and R. P. Rand. 1983. Membrane interaction and deformation. *Ann. NY Acad. Sci.* 416:1–12.
20. Lis, L. J., M. McAlister, N. L. Fuller, R. P. Rand, and V. A. Parsegian. 1982. Interactions between neutral phospholipid bilayer membranes. *Biophys. J.* 37:657–666.
21. Evans, E., and D. Needham. 1986. Giant vesicle bilayers composed of mixed lipids, cholesterol, and polypeptides: thermo-mechanical and (mutual) adherence properties. *Farad. Soc.* In press.
22. Verkleij, A. J. C., J. Mombers, L. Leunissen-Bijvelt, and P. Ververgaert. 1979. Lipidic intermembraneous particles. *Nature (Lond.)*. 279:162–163.
23. Siegel, D. 1984. Inverted micellar structures in bilayer membranes. Formation rates and half-lives. *Biophys. J.* 45:399–420.
24. Bearer, E. L., N. Duzgunes, D. S. Friend, and D. Papahadjopoulos. 1983. Fusion of phospholipid vesicles arrested by quick freezing. The question of lipidic particles as intermediates in membrane fusion. *Biochim. Biophys. Acta*. 693:93–98.